ISBN: 978-628-96613-3-0. ISSN: 2414-6390. Digital Object Identifier: https://dx.doi.org/10.18687/LACCEI2026.1.1.1589

Impact of Manufacturing Methods on the Aerodynamic Performance of the SG6043 Airfoil: An Experimental Comparison

Maximino Jiménez-Ceciliano[1]; Juan José Montero-Jiménez[2]; Gustavo Richmond-Navarro[3], Williams Calderón-Muñoz[4]; Takanori Uchida[5]; José Miguel Sánchez-De-La-Hoz[6]; Miguel Fernando Montoya-Vallejo[7]
[1,2,3] Tecnológico de Costa Rica, Costa Rica, *maxjimenez@itcr.ac.cr*, *grichmond@itcr.ac.cr*, *juan.montero@itcr.ac.cr*
[4] Universidad de Chile, *wicalder@uchile.cl*
[5] Kyushu University, *takanori@riam.kyushu-u.ac.jp*
[6] Universidad de la Costa, *jmiguelsanchez@mail.uniatlantico.edu.co*
[7] Escuela Colombiana de Ingeniería Julio Garavito, *miguel.montoyav@escuelaing.edu.co*

Abstract– Prototyping is a fundamental tool in airfoil design and aerodynamic research, enabling rapid evaluation of geometry, manufacturing constraints, and performance through experimental testing. Among commonly used prototyping techniques, laser cutting and fused deposition modeling (FDM) are widely adopted in airfoil development. This paper presents an experimental comparison of two prototyping manufacturing methods applied to SG6043 airfoil models for small-scale wind turbines operating under low wind speed conditions. The airfoils were fabricated using laser cutting with medium-density fiberboard (MDF) and FDM with polyethylene terephthalate glycol-modified (PETG). Their aerodynamic performance was assessed in a wind tunnel, focusing on lift, drag, and lift-to-drag (L/D) ratio. Experimental results show that the FDM-manufactured airfoil outperforms the laser-cut prototype, achieving an L/D ratio approximately 20% higher. These findings highlight the influence of prototyping methods and material selection on airfoil aerodynamic performance and support the use of FDM for rapid prototyping in airfoil design and research.

Keywords- Wind tunnel, SG6043 Airfoil, Wind turbine, Rotor, Prototyping.

I. Introduction

The purpose of a prototype is to approximate one or more characteristics of a product in order to validate requirements, identify design issues, and optimize performance through testing and parameter manipulation [1], [2], [3]. In the field of airfoil research, rapid prototyping has become an essential tool for the experimental evaluation of different airfoil configurations, enabling faster assessment of aerodynamic behavior and significantly reducing product development time in the energy sector [4].

Among the various prototyping techniques currently employed, fused deposition modeling (FDM), commonly referred to as 3D printing, has gained widespread adoption due to its ability to produce rapid and cost-effective prototypes using a wide range of polymeric materials while maintaining high reproducibility [5], [6]. Previous experimental studies have demonstrated the suitability of FDM for aerodynamic applications; for instance, Oliveira et al. [7] investigated small wind turbines manufactured using FDM and reported satisfactory agreement between experimental torque and power measurements and analytical predictions.

Laser cutting represents another widely used prototyping technique, particularly valued for its precision, robustness, and manufacturing speed, making it a competitive alternative for the fabrication of aerodynamic models and experimental prototypes [8].

Regarding FDM materials, polylactic acid (PLA), polyethylene terephthalate glycol-modified (PETG), and acrylonitrile butadiene styrene (ABS) are among the most commonly used polymers for prototype manufacturing [9], [10]. PLA and ABS have been extensively applied in the prototyping of aerodynamic profiles and small-scale wind turbines, with PLA exhibiting favorable structural performance in several studies [10], [11]. In contrast, PETG has received comparatively limited attention in airfoil prototyping applications, despite its advantageous mechanical properties and improved surface finish when compared to other thermoplastic materials [12]. This gap highlights PETG as a relevant material for further investigation in aerodynamic prototyping studies.

In laser cutting–based rapid prototyping, commonly used materials include wood-based products such as medium-density fiberboard (MDF), as well as metals such as titanium and stainless steel [13]. However, MDF has been scarcely reported in the literature for the fabrication of airfoil prototypes. Its advantageous properties include low cost, ease of machining, and favorable mechanical and physical characteristics. This makes MDF a interesting alternative for airfoil manufacturing [14].

A wide variety of airfoil geometries have been extensively investigated in the literature. Notable examples include studies on airfoil families such as NACA, FX, and S, which were systematically analyzed in previous research [15]. In addition, airfoils specifically designed for small-scale wind turbines with rated capacities between 1 and 5 kW have been developed. This group includes the SG6040 airfoil and the three primary members of the S-series: SG6041, SG6042, and SG6043 [16]. Among these, the SG6043 airfoil has been widely studied and has demonstrated strong aerodynamic performance, particularly in regions characterized by low wind speed conditions [17].

The objective of this study is to evaluate the aerodynamic performance of the SG6043 airfoil fabricated using two different manufacturing methods. The SG6043 profile was selected due to its proven suitability for small-scale wind turbine applications [18]. Two types of prototypes were manufactured: one using fused deposition modeling (FDM) and the other using laser cutting. The aerodynamic performance of both airfoils was experimentally evaluated and compared in a wind tunnel under a constant wind speed of 10.5 m/s. The findings of this work aim to contribute to the optimization of airfoil prototyping strategies and to the improvement of aerodynamic efficiency in small-scale wind turbine applications.

II. Materials and methods

To achieve the objectives of this study, SG6043 airfoil prototypes were manufactured using two different fabrication methods. Airfoils made of polyethylene terephthalate glycol-modified (PETG) were produced using the fused deposition modeling (FDM) process, while airfoils made of medium-density fiberboard (MDF) were fabricated by assembling laser-cut sheets of this material. The aerodynamic performance of both prototypes was experimentally evaluated in a wind tunnel to determine lift and drag forces at different angles of attack (AoA).

A. FDM Manufacturing Process

The polymer-based airfoils were fabricated using a Cartesian 3D printer [19], as shown in Fig. 1. PETG filament with a nominal diameter of 1.75 ± 0.05 mm was used. According to the manufacturer's specifications, the recommended extrusion temperature for PETG ranges from 230 °C to 260 °C.

To determine the optimal printing temperature, a preliminary temperature calibration test was conducted using a temperature tower. A temperature range from 200°C to 255°C was evaluated in increments of 5 °C. Fig. 2 shows the experimental results of the printing temperature y which the 210°C was selected. The final printing parameters adopted for the fabrication of the airfoils are listed in Table I.

After printing, a post-processing step consisting of manual sanding was applied to all FDM-manufactured airfoils in order to reduce surface irregularities and improve surface finish.

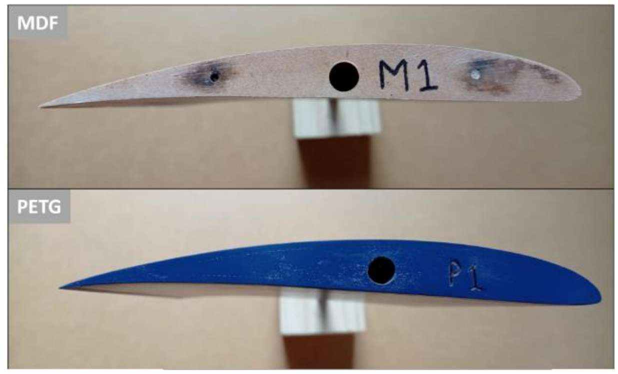

Fig 1. MDF and PETG airfoil prototypes.

TABLE I
PETG FILAMENT PRITING PARAMETERS

Parameter	Value
Printing Temperature	210C
Build Plate Temperature	70C
Layer Height	0,16mm
Line Width	0,4mm
Wall Thickness	1,6mm
Wall Line Count	4
Infill Density	25%
Infill Overlap Percentage	30%
Print Speed	45mm/s
Retraction Distance	5mm
Retraction Speed	45mm/s
Fan Speed	100%
Build Plate Adhesion Type	Raft

B. Laser-Cut MDF Manufacturing Process

For the fabrication of the MDF airfoils, 3 mm thick sheets were used. The sheets were cut using a laser cutting process and subsequently assembled using white adhesive until the target airfoil width of 150 mm was achieved. To ensure alignment and structural rigidity, two 3/8-inch steel rods were incorporated into the assembly, as illustrated in Fig. 1.

As with the FDM prototypes, a surface finishing process involving sanding was performed to eliminate surface imperfections and ensure consistency between specimens. After assembly, surface gaps between MDF layers were filled using wood filler prior to sanding. Multiple sanding stages were applied using progressively finer grit sizes to achieve a uniform surface finish. This finishing process represents a significant of the fabrication time, turning out in a larger manufacturing duration compared to FDM.

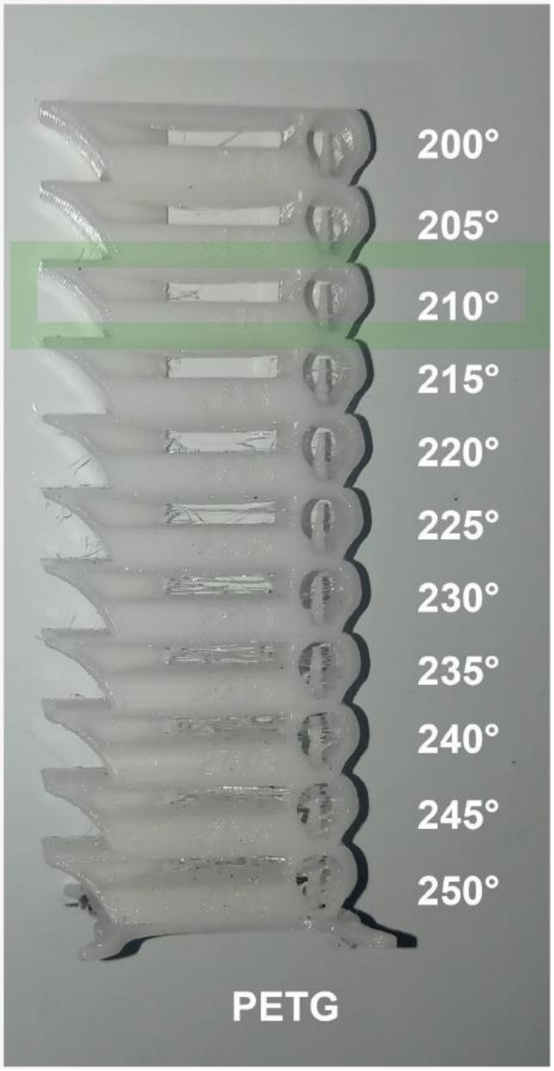

Fig 2. Printing temperature test for PETG material.

C. Geometric Modeling

The airfoils manufactured using FDM were modeled using SolidWorks 2022, while AutoCAD 2022 was employed for the design of the MDF-based prototypes. In both cases, the models were generated based on the SG6043 aerodynamic profile obtained from [20]. All airfoils were designed with a chord length of 150 mm and a span (width) of 150 mm, ensuring identical geometric characteristics for both manufacturing methods.

D. Wind Tunnel Experimental Setup

The aerodynamic tests were conducted in an open-circuit axial wind tunnel, previously described by Garro-Fernández et al. [21], as shown in Fig. 3. The wind tunnel is equipped with an axial fan driven by a 1 hp electric motor and features a square test section with dimensions of 30 × 30 cm (Fig. 4).

Fig 3. Wind tunnel used to the prototype test.

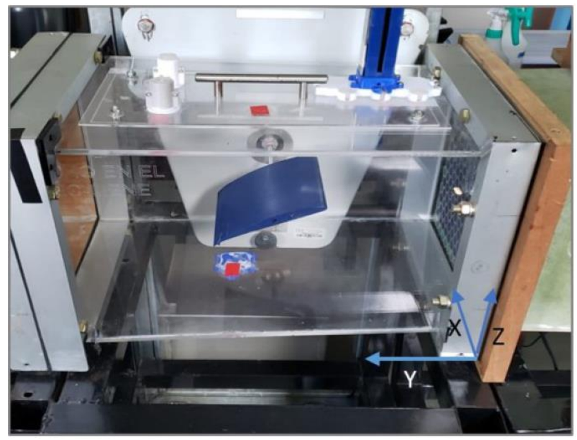

Fig 4. Experimental setup for aerodynamic testing of the SG6043 airfoil.

The dimensions of the airfoil models were selected such that the blockage ratio did not exceed 10% of the test section area, in accordance with established wind tunnel testing guidelines [22]. Lift and drag forces were measured using a single-component force balance (Tecquipment AF1300Z). To attach the airfoil to the balance, a 5/16-inch hole was drilled at the centroid of each profile, as shown in Fig. 1 and Fig. 4.

Force measurements were recorded over a 60 s interval for each test condition. This duration was determined through preliminary tests to ensure time independence of the measured forces. Data were acquired at a maximum sampling frequency of 2 Hz, which corresponds to the maximum allowable frequency of the data acquisition system.

E. Test Conditions and Data Processing

For each airfoil and AoA, a total of 120 data points were collected. Preliminary analysis of the raw force measurements revealed deviations from normality and non-constant variance, particularly at higher angles of attack. For this reason, a Box–Cox transformation was applied prior to statistical analysis [23]. After transformation, mean values and standard deviations were computed for each AoA.

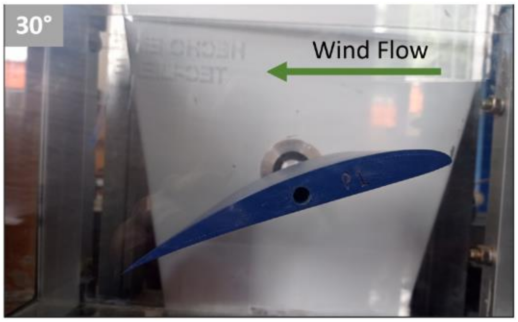

Fig 5. Experimental setup at an angle of attack (AoA) of 30°.

All experiments were conducted at a constant free-stream wind speed of 10.5 m/s, corresponding to a Reynolds number of approximately 1.05×10^5, calculated using equation (1)

$$Re = \frac{V\,d}{\nu} \quad (1)$$

where V is the free-stream velocity, d =0.15 m is the chord length, and $\nu=1.5\times10^{-5} m^2/s$ is the kinematic viscosity of air. This Reynolds number is representative of operating conditions commonly encountered in small-scale wind turbine applications [24].

The angle of attack ranged from −25° to 50°, with increments of 5°. An example of the airfoil orientation at 30° AoA is shown in Fig. 5. Lift and drag forces were measured at each orientation angle, as summarized in Table II. To minimize experimental bias, measurements were conducted in a randomized order.

F. Scope and Limitations

This study focuses on a comparative experimental analysis of two-dimensional (2D) SG6043 airfoil models, defined as geometries with no variation along the spanwise direction. The evaluation of complete wind turbine rotors is beyond the scope of this work and will be addressed in future studies.

Although the airfoil models have a finite span and an aspect ratio close to 1, the present study emphasizes a comparative assessment of aerodynamic performance rather than the determination of absolute two-dimensional airfoil coefficients. While aerodynamic forces are directly reported, nondimensional coefficients (CL and CD) were not included. This limits direct comparison with external databases and literature, although it does not affect the internal comparison between prototypes.

All tests were conducted at a single Reynolds number ($Re \approx 1.05\times10^5$), corresponding to low wind speed conditions typical of small-scale wind turbines. Therefore, the results are valid within this flow regime, and their generalization to other Reynolds numbers, airfoil geometries, or higher aspect ratios requires further experimental validation.

TABLE II
NUMBER OF WIND TUNNEL TESTS PERFOMED FOR EACH EXPERIMENTAL VARIABLE

Variable	**Posible value**	**Number of options**
Forces (N)	Drag and lift	2
Airfoil material	MDF, PETG	2
Angle of Attack (°)	-25, -20, -15, -10, -5, 0, 5, 10, 15, 20, 25, 30, 35, 40, 45, 50	16
Total of tests		64

Although both prototypes were subjected to similar surface finishing processes, no quantitative surface roughness characterization (e.g., Ra or Rz parameters) was performed. As discussed in the results section, surface roughness may influence boundary layer development, lift generation, and stall behavior. However, due to the lack of direct measurements, the relationship between roughness and aerodynamic performance could not be conclusively established.

No wind tunnel correction factors (e.g., blockage or wall interference corrections) were applied, despite the blockage ratio remaining below 10%. This may introduce systematic deviations in the absolute force values. However, since all experiments were conducted under identical conditions, the comparative validity between both manufacturing methods is maintained.

Although statistical preprocessing techniques such as the Box–Cox transformation were applied, uncertainty propagation was not extended to derived quantities such as the lift-to-drag (L/D) ratio. Therefore, variability in L/D is not explicitly quantified through confidence intervals, which limits the statistical interpretation of aerodynamic efficiency differences.

Finally, while differences in aerodynamic performance are discussed in terms of boundary layer behavior and stall characteristics, no direct flow visualization or boundary layer measurements were conducted. Additional experimental techniques, such as tuft visualization or smoke flow analysis, would be required to better understand the underlying fluid dynamic mechanisms.

III. RESULTS AND DISCUSSION

The lift and drag force measurements obtained for the SG6043 airfoil manufactured using PETG through fused deposition modeling (FDM) and MDF through laser cutting are presented in Tables III and IV, respectively. Each table includes the corresponding standard deviations, calculated after applying the Box–Cox transformation and averaging the processed data. The results are reported as a function of the angle of attack

(AoA) at which the airfoil was positioned in the wind tunnel test section. A graphical representation of the lift force, drag force, and lift-to-drag (L/D) ratio is shown in Fig. 6.

As illustrated in Fig. 6(c), the airfoil manufactured using FDM exhibits a consistently higher L/D ratio than the laser-cut MDF airfoil across the evaluated AoA range. Although the drag forces measured for both airfoils show only minor differences (Fig. 6(b)), with an average standard deviation of approximately 0.002 N, the lift force generated by the FDM airfoil is systematically higher at all tested angles (Fig. 6(a)), with an average standard deviation of approximately 0.003 N. Notably, at no AoA does the lower confidence limit of the PETG airfoil overlap with the upper confidence limit of the MDF airfoil, resulting in a clear advantage in aerodynamic efficiency for the FDM-manufactured prototype.

The maximum aerodynamic efficiency for both manufacturing methods occurs at an AoA between 5° and 10°, which corresponds to the optimal performance region of the SG6043 airfoil and is consistent with previously reported results [18]. Within this AoA range, the FDM-manufactured airfoil achieves an L/D ratio approximately 20% higher than that of the laser-cut MDF airfoil. At an AoA of −5°, the difference in L/D ratio between both airfoils is close to two units, further highlighting the superior performance of the FDM prototype.

The observed trends in lift, drag, and optimal angle of attack are consistent with previously published experimental and numerical results for the SG6043 airfoil at similar Reynolds numbers, such as those reported by [24]. This agreement provides additional validation of the experimental methodology employed in this study.

These differences can be partially attributed to the distinct characteristics of the manufacturing methods and raw materials. FDM-based polymer printing provides a more homogeneous and repeatable fabrication process within a relatively short production time. However, the mechanical and aerodynamic performance of FDM-manufactured airfoils is strongly influenced by printing parameters such as extrusion temperature, layer height, and infill density. Consequently, careful selection and optimization of these parameters are essential, particularly when the airfoil is subjected to extensive experimental testing.

In contrast, the fabrication of airfoils using laser cutting involves a longer manufacturing process and requires additional surface finishing steps, including sanding and correction of surface imperfections, in order to achieve dimensional uniformity comparable to that obtained through FDM. The total manufacturing times for each airfoil are summarized in Table V, illustrating the differences in production efficiency between both methods.

TABLE III
DRAG FORCE AND STANDARD DEVIATION (DEV) FOR EACH AIRFOIL PROTOTYPE AT DIFFERENT ANGLES OF ATTACK (AOA)

AoA [°]	**PETG Airfoil Lift [N]**	**DEV PETG**	**MDF Airfoil Lift [N]**	**DEV MDF**
-25	-0,509	0,016	-0,578	0,018
-20	-0,398	0,013	-0,507	0,013
-15	-0,296	0,013	-0,398	0,010
-10	-0,033	0,012	-0,194	0,012
-5	0,15	0,013	0,004	0,012
0	0,379	0,010	0,183	0,011
5	0,619	0,008	0,418	0,009
10	0,871	0,009	0,675	0,013
15	1,1740	0,011	0,939	0,012
20	1,524	0,014	1,241	0,014
25	1,727	0,012	1,486	0,010
30	1,951	0,015	1,65	0,013
35	1,616	0,015	1,516	0,019
40	1,406	0,018	1,275	0,016
45	1,439	0,020	1,213	0,015
50	1,320	0,017	1,188	0,023

TABLE IV
LIFT FORCE AND STANDARD DEVIATION (DEV) FOR EACH AIRFOIL PROTOTYPE AT DIFFERENT ANGLES OF ATTACK (AOA)

AoA [°]	**PETG Airfoil Lift [N]**	**DEV PETG**	**MDF Airfoil Lift [N]**	**DEV MDF**
-25	0,439	0,012	0,424	0,013
-20	0,308	0,007	0,33	0,008
-15	0,216	0,011	0,23	0,008
-10	0,15	0,01	0,131	0,01
-5	0,079	0,011	0,063	0,012
0	0,11	0,01	0,07	0,01
5	0,131	0,01	0,105	0,011
10	0,181	0,014	0,148	0,013
15	0,292	0,01	0,256	0,009
20	0,4	0,01	0,378	0,009
25	0,567	0,013	0,54	0,008
30	0,695	0,009	0,698	0,01
35	0,999	0,012	0,963	0,012
40	1,075	0,011	1,049	0,01
45	1,273	0,012	1,23	0,013
50	1,49	0,016	1,427	0,013

TABLE V
MANUFACTURING TIME FOR SG6043 AIRFOIL PROTOTYPES FABRICATED USING DIFFERENT METHODS

Material	Manufacturing method	Fabrication Time (h)
PETG	FDM	14
MDF	Laser Cut	60

As the AoA increases, the aerodynamic performance of both airfoils exhibits noticeable changes, particularly near an AoA of 30°, where stall occurs for both PETG and MDF airfoils, as shown in Fig. 6(a). The reduction in lift is more abrupt for the FDM-manufactured airfoil (P1), suggesting that surface characteristics, such as roughness, may influence the onset of stall. However, establishing a direct correlation between surface roughness and stall behavior remains challenging, as boundary layer separation plays a dominant role in this phenomenon.

Prior to stall, differences in boundary layer thickness between the two airfoils are inferred from the observed lift behavior, which may be attributed to the distinct material properties and surface conditions associated with each manufacturing method.

These observations indicate that, while surface roughness and fabrication processes affect aerodynamic performance, boundary layer dynamics are also critical contributing factors.

Therefore, future studies focusing on detailed boundary layer analysis, particularly near stall conditions, would provide deeper insight into the aerodynamic mechanisms governing the performance of additively manufactured and laser-cut airfoil prototypes. Such investigations would not only clarify the influence of manufacturing techniques but also contribute to the optimization of small-scale wind turbine designs.

IV. CONCLUSIONS AND FUTURE WORK PERSPECTIVES

This study investigated the influence of prototyping manufacturing methods on the aerodynamic performance of SG6043 airfoil prototypes intended for small-scale wind turbine applications operating under low Reynolds number conditions. Two fabrication approaches were experimentally evaluated: fused deposition modeling (FDM) using PETG and laser cutting using medium-density fiberboard (MDF). The results obtained from wind tunnel testing demonstrate that the manufacturing method plays a significant role in the aerodynamic behavior of airfoil prototypes.

The FDM-manufactured airfoil consistently exhibited higher lift values and superior aerodynamic efficiency than the laser-cut MDF airfoil across the entire range of tested angles of attack. In particular, the lift-to-drag (L/D) ratio of the FDM prototype was approximately 20% higher within the optimal performance region, which occurred between 5° and 10° angle of attack. This performance trend is consistent with previously reported aerodynamic characteristics of the SG6043 airfoil and confirms the suitability of FDM-based prototyping for experimental airfoil research.

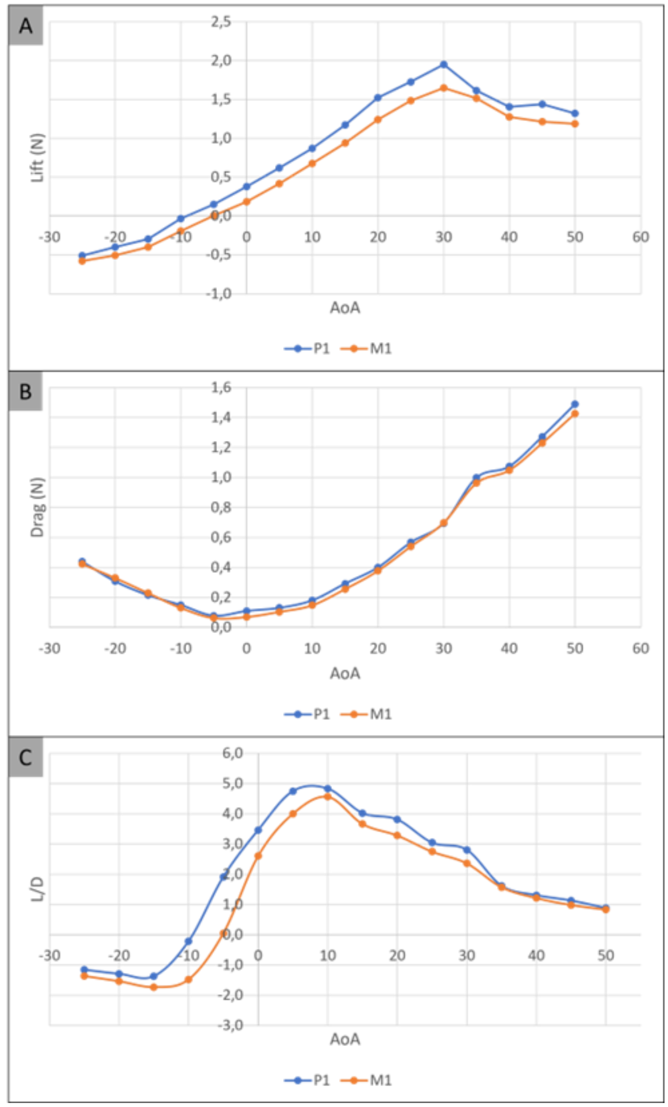

Fig 6. Aerodynamic performance of SG6043 airfoils fabricated using different manufacturing methods: P1 (FDM–PETG) and M1 (laser-cut MDF).

These findings highlight the advantages of FDM as a rapid prototyping technique for airfoil design and aerodynamic research, especially in terms of reproducibility, manufacturing efficiency, and aerodynamic performance. The results also suggest that material selection and surface characteristics associated with the prototyping method can influence boundary layer behavior and stall onset, particularly at higher angles of attack.

Future work will focus on extending the present analysis to include detailed boundary layer characterization and the evaluation of flow control strategies applied to additively manufactured airfoils. In addition, further investigations will explore the influence of FDM process parameters, such as layer height and surface finishing, on surface roughness and their subsequent impact on aerodynamic performance. These studies will contribute to the optimization of rapid prototyping methodologies for the development of efficient small-scale wind turbine components.

Declaration of the Use of Generative AI and AI-Assisted Technologies in the Writing Process

During the preparation of this work the authors used ChatGPT in order to check clarity and correctness of English language. After using this tool/service, the authors reviewed and edited the content as needed and take full responsibility for the content of the publication.

Acknowledgment

The authors express their gratitude to the Instituto Tecnológico de Costa Rica and the Vicerrectoría de Investigación y Extensión for providing partial financial support for this research through project 1341-020. Special thanks are extended to the LIENE: Wind Energy Research Laboratory for their technical support, as well as to Juan Luis Crespo Mario, Iván Araya Meneses, and Gustavo Murillo Zumbado for their valuable contributions to this work.

References

[1] B. Camburn *et al.*, "Design prototyping methods: State of the art in strategies, techniques, and guidelines," *Design Science*, vol. 3, pp. 1–33, 2017.

[2] V. Kumar and J. Linsey, "Build to learn: Effective strategies to train tomorrow's designers," in *ASEE Annual Conference and Exposition*, 2012.

[3] R. Anderl, K. Mecke, and L. Klug, "Advanced Prototyping With Parametric Prototypes," in *Digital Enterprise Technology*, Springer, Boston, MA, 2007, pp. 503–510. doi: 10.1007/978-0-387-49864-5_59.

[4] S. Daneshmand, A. Ahmadi, and C. Aghanajafi, "Evaluation of FDM Rapid Prototyping with ABSi Material for Airfoil Design," *Energy Procedia*, vol. 160, pp. 777–782, 2008.

[5] U. Goltenbott, Y. Ohya, S. Yoshida, and P. Jamieson, "Aerodynamic interaction of diffuser augmented wind turbines in multi-rotor systems," *Renew. Energy*, vol. 112, pp. 25–34, 2017.

[6] U. Jai, "Additive Manufacturing in Aerospace Industry," in *Conference Proceedings of the Advanced Manufacturing Student Conference*, 2022.

[7] S. Oliveira, A. Vagtinski, J. Luz, T. Jodar, and A. Prisco, "Experimental Evaluation of the Aerodynamic Performance of Small Wind Turbines Confectioned in 3D Prototyping," *Thermal Engineering*, vol. 15, pp. 15–23, 2016.

[8] S. Kohtala and M. Steinert, "From Hand-Drawn Sketching to Laser Cutting - A Proof of Concept Prototype and Pilot Study," in *International Conference on Engineering Design*, Delft, 2019.

[9] D. Arup and N. Yodo, "A Systematic Survey of FDM Process Parameter Optimization and Their Influence on Part Characteristics," *Manufacturing and Materials Processing*, vol. 64, p. 30, 2019.

[10] S. Arivalagan, R. Sappani, R. Cep, and M. Kumar, "Optimization and Experimental Investigation of 3D Printed Micro Wind Turbine Blade Made of PLA Material," *Materials*, p. 22, 2023.

[11] K. Bassett, R. Carriveau, and D. Ting, "3D printed wind turbines part 1: Design considerations and rapid manufacture potential," *Sustainable Energy Technologies and Assessments*, vol. 11, pp. 186–193, 2015.

[12] D. Chauhan and M. Chudasama, "Effect of Process Parameters on Different Properties of 3D Printed PETG Parts Prepared Using FDM," *International Journal of Advanced Research in Science, Communication and Technology*, vol. 2, pp. 672–678, 2022.

[13] K. Naresh and P. Khatak, "Laser cutting technique: A literature review," *Mater. Today Proc.*, vol. 56, pp. 2484–2489, 2021.

[14] L. Chuan, N. A. S. M. Puad, M. Selimin, N. Manap, H. Abdullah, and M. Idris, "An overview on development of environmental friendly medium density fibreboard," *Mater. Today Proc.*, vol. 29, pp. 52–57, 2020.

[15] M. N. Kaya, A. Kok, and H. Kurt, "Comparison of Aerodynamic Performances of Various Airfoils from Different Airfoil Families Using CFD," *Wind and Structures*, vol. 32, no. 3, pp. 239–248, 2021.

[16] P. Giguere and M. Selig, "New airfoils for small horizontal axis wind turbines," *J. Sol. Energy Eng.*, vol. 120, no. 2, pp. 108–114, 1998.

[17] P. Arumugam, V. Ramalingam, and K. Bhaganagar, "A pathway towards sustainable development of small capacity horizontal axis wind turbines: Identification of influencing design parameters and their role on performance analysis," *Sustainable Energy Technologies and Assessments*, vol. 44, 2021.

[18] G. Richmond-Navarro, M. Montenegro-Montero, and C. Otrola, "Revisión de los perfiles aerodinámicos apropiados para turbinas eólicas de eje horizontal y de pequeña escala en zonas boscosas," *Rev. Lasallista Investig.*, vol. 17, pp. 233–244, 2020.

[19] Artillery3D, "Artillery Sidewinder X1," 2023.

[20] AirfoilTools, "SG6043 (sg6043-il) Airfoil," 2023.

[21] F. Garro-Fernández, C. A. Echandi-Jara, E. Fallas-Hernández, M. Zúñiga-Pepper, and G. Richmond-Navarro, "Diseño y construcción de un túnel de viento subsónico de circuito abierto," *Revista Tecnología en Marcha*, vol. 38, no. 1, pp. 128–144, 2025, doi: 10.18845/tm.v38i1.7051.

[22] J. B. Barlow, W. H. Rae, and A. Pope, *Low-Speed Wind Tunnel Testing*. John Wiley & Sons, 1999.

[23] R. Sakia, "The Box-Cox transformation technique: a review," *Journal of the Royal Statistical Society: Series D (The Statistician)*, vol. 41, no. 2, pp. 169–178, 1992.

[24] G. Richmond-Navarro, T. Uchida, and W. R. Calderón-Muñoz, "Shrouded wind turbine performance in yawed turbulent flow conditions," *Wind Engineering*, vol. 46, no. 2, 2021.